

MEASURING ATMOSPHERIC SCATTERING FROM DIGITAL IMAGE SEQUENCES

Tarek El-Gaaly and Joshua Gluckman

Computer Science Department, The American University in Cairo, Egypt

Keywords: Atmospheric scattering, Haze, Image, Dehazing, Depthmap.

Abstract: Current environmental monitoring devices are limited in their capability of measuring atmospheric particulate matter (PM) over large areas. Quantifying the visual degrading effects of atmospheric scattering in digital images of urban scenery and correlating these effects to PM levels is a vital step in more practically monitoring our environment. Currently, image haze removal (or dehazing) techniques exist which remove all the haze from a scene for the sole purpose of enhancing vision. This paper presents an extension to existing dehazing algorithms to use sequences of images captured over time and enforce a constant depth constraint. An experimental comparison of dehazing algorithms is then presented in the context of measuring atmospheric scattering and depth recovery using both simulation and depth measurements from real data.

1 INTRODUCTION

How air pollution affects the visual appearance of scenes has been a research challenge for scientists. Changes in emissions, urban growth, and many other factors influence the amount and type of air pollution. Suspended particulate matter (PM) in the atmosphere visually degrades urban scenery. Understanding the visual effects of the atmosphere over large urban areas captured in ground-based digital images is a vital step in measuring global levels of PM over large areas more practically.

Atmospheric scattering fluctuates proportionally to the level of PM in the atmosphere (Vollmer, 2003; Jacobson, 2005; Kokhanovsky, 2003) and therefore offers a way of measuring PM through visual means. The challenge of measuring atmospheric scattering visually lies in finding the relationship between image pixel intensities and atmospheric scattering taking place in the scene. The difficulty of finding this relationship lies in accounting for the many factors that affect the pixel values, such as: physical scattering of light by molecules and suspended particles, position of the sun, geometric and radiometric camera calibration, multiple-scattering, ground and object reflection, the presence of non-spherical particles and variations in background scene radiance due to changes in illumination (Kokhanovsky, 2003; Jacobson, 2005).

Currently, haze removal (or dehazing) algorithms exist which remove most of the haze in a scene. This

is ideal from the perspective of enhancing vision but finding the relationship between the extracted haze and global PM levels from ground-based images is an under researched problem.

In the context of measuring atmospheric scattering visually, three existing dehazing algorithms are analyzed and compared. The first is a polarization-based dehazing method (Schechner et al., 2003; Shwartz et al., 2006). Two or more images are captured with different degrees of polarization (using a polarizer filter). The second is the dichromatic framework (Narasimhan and Nayar, 2000) which dehazes using multiple images of the same scene under different weather conditions. The third dehazing algorithm is a more recent approach which uses a statistical prior called the 'Dark Channel' to dehaze a single image (He et al., 2009). This prior is based on observed statistics of outdoor images free of haze. It is based on the observation that the majority of local patches in outdoor haze-free images contain pixels which have very low intensities in at least one color channel. Other more recent methods which emerged through the course of this research are: single image dehazing (Fattal, 2008) and visibility in bad weather from a single image (Tan, 2008). The latter uses the observation that haze-free images naturally have higher contrast and hence dehazing is done by maximizing the local contrast. Fattal assumes that atmospheric transmission and surface shading are locally uncorrelated.

Some methods exist which require additional information, such as (Kopf et al., 2008; Narasimhan and Nayar, 2003). These methods require additional depth knowledge of the scene.

The first contribution of this research is the extension of existing dehazing algorithms to use sequences of images captured over time. An optimization algorithm enforces a constant depth constraint over the sequence of images and allows the decomposition of the scene into a sequence of atmospheric scattering coefficients and a relative depthmap. The second contribution is an experimental comparison of dehazing algorithms, in the context of measuring atmospheric scattering and depth recovery, using both simulation and depth measurements from real data.

2 BACKGROUND

In computer vision and graphics, the widely used model for describing the formation of haze in images is as follows (Tan, 2008; Fattal, 2008; Narasimhan and Nayar, 2000; Narasimhan and Nayar, 2002):

$$I = Re^{-\beta z} + A_{\infty}(1 - e^{-\beta z}) \quad (1)$$

where I is the observed image intensity, R is the scene radiance, A_{∞} is the global atmospheric airlight, β is the atmospheric scattering coefficient and z is the depth of the scene. The term $e^{-\beta z}$ represents the medium transmission describing the fraction of light that is not scattered as it passes through the medium. This model assumes a homogeneous atmosphere.

The term $Re^{-\beta z}$ of equation 1 is known as the direct transmission, and the second term $A_{\infty}(1 - e^{-\beta z})$ is known as airlight. Direct transmission is the part of scene radiance that eventually reaches the viewpoint after suffering attenuation as it passes through the medium. Airlight results from light scattered by the medium towards the viewpoint and causes an increase in brightness as the depth of the scene increases.

This research focuses on three existing dehazing methods. Each of them dehaze an image of a scene and produce a relative depthmap scaled to the atmospheric scattering coefficient β (in equation 1). The polarization-based dehazing method uses a sequence of two or more images captured with different degrees of polarization. The degree of polarization is varied by varying the angle of a polarizer filter attached to a camera. Using the difference in intensity of airlight between the images and the haze image model (equation 1) the scene is dehazed and a depthmap is produced. The 'Dichromatic Framework' measures atmospheric scattering using changes in weather condi-

tions. The color of a scene point is modeled as a linear combination of direct transmission and airlight vectors in a color space. The color of a scene point may vary anywhere within the plane (dichromatic plane) defined by the vectors. The 'Dark Channel' method uses a statistical prior to dehaze a haze-filled input image. It uses the observation that outdoor haze-filled images are composed of local patches which contain pixels with very low intensity in at least one color channel. This is due to the overwhelming presence of shadows, colorful surfaces and dark surfaces.

3 CONSTANT DEPTH CONSTRAINT

The Constant Depth Constraint (CDC) is based on the fact that the scene being captured in the form of images over time has constant depth. This algorithm is based on the haze image model (equation 1). The model is rewritten as follows:

$$\begin{aligned} I_i^c(x) &= R^c(x)T_i(x) + A^c(1 - T_i(x)) \quad (2) \\ T_i(x) &= e^{-\beta_i z(x)} \quad (3) \end{aligned}$$

The superscript signifies that the coefficient is defined over the three color channels (RGB). The subscript signifies that the variable varies over time. $T_i(x)$ is the global transmittance of each image captured at time i . x is the spatial index corresponding to square patches over the images. The scene radiance $R^c(x)$ varies as the illumination due to the sun in the scene changes direction. This variation is assumed to be small over the limited period of time the sequence of images are captured over (see Figure 2). In addition to this assumption, we performed a normalization technique on the sequence of images captured of the same scene. We choose a flat surface in the scene and normalized our radiance measurements by the radiance of this surface. As the illumination changes in the scene, the radiance of this flat surface varies with it and by using this to normalize the scene radiance of each image we essentially factor out the variation between the sequence of images. The flat surface chosen in the scene can be seen in Figure 1.

The CDC constraint is used to form an optimization algorithm to recover a sequence of atmospheric scattering coefficients corresponding to the sequence of images captured over time and one single depthmap of the scene. The algorithm is based on the relation between the transmittance, atmospheric scattering and depth in equation 3 under the constraint of constant depth of the scene (CDC). This



Figure 1: The flat surface of the scene used to normalize the radiance of each image and therefore account for the change in illumination. It can be seen in the lower left hand side of the scene.

optimization algorithm extends the existing dehazing techniques. The CDC improves the accuracy of the relative depthmap recovered by each dehazing technique by factoring the scaled depthmap into a set of atmospheric scattering coefficients (one for each image) and one single depthmap, no longer scaled by the atmospheric scattering coefficient.

A solution is found by implementing a standard least squares regression to find the best fit variables in the transmittance model (equation 3). Accordingly, equation 3 yields the following error function to minimize:

$$\varepsilon = \sum_i \sum_x [\beta_i z(x) - \log(T_i(x))]^2 \quad (4)$$

Taking the partial derivatives $\partial\varepsilon/\partial\beta_i$ and $\partial\varepsilon/\partial z(x)$ of the equation above and setting the derivatives to zero results in the two equations:

$$\beta_i = \frac{\sum_x T_i(x) z(x)}{\sum_x (\beta_i)^2} \quad (5)$$

$$z(x) = \frac{\sum_i T_i(x) \beta_i}{\sum_i (\beta_i)^2} \quad (6)$$

Using the above equations we are able to repeatedly iterate between solving for β_i and then solving for $z(x)$ until they converge.

The algorithm for this optimization is as follows:

```

For each patch
  while delta of Beta is not close to 0
    Beta <- min(Beta,1)
    Beta <- max(Beta,0)
    z <- max(z,0)
    Compute Beta using equation 5
    Clamp Beta of image with
      maximum atmospheric airlight to 1
    Compute z using equation 6
  end
end

```

end
end

As there may be multiple possible solutions in the solution space, the maximum atmospheric scattering coefficient of the sequence of images is clamped to 1 and all other scattering coefficients are scaled with respect to it. The maximum scattering coefficient is chosen as the brightest image (i.e. the image with the maximum atmospheric airlight intensity measured from the low sky region). In addition to this the depth is clamped above 0 to avoid negative depth estimates. The scattering coefficients are also clamped to values between 0 and 1.

The algorithm described above converges to an unscaled relative depthmap and a set of scattering coefficients (one per image). This optimization extends existing dehazing algorithms and allows the accuracy of the measured scattering coefficients and the recovered depthmap to be compared. This algorithm converges to a depthmap no longer scaled by the atmospheric scattering coefficient and therefore is more accurate. There are two benefits of this optimization model. From the perspective of atmospheric scattering, an estimate of the atmospheric scattering coefficients for each captured image is derived by applying our model to a sequence of images of the same scene, as seen in Figure 2. From the point of view of the accuracy of the recovered relative depthmap the accuracy is increased by factoring out the scattering coefficient scaling factor.

4 EXPERIMENTAL RESULTS

The existing dehazing algorithms were compared in the context of atmospheric scattering measurement by extending each algorithm with the CDC optimization and applying them to simulated haze images. We used the model of haze described in equation 1 to synthesize simulated haze scenes. We injected errors into different parameters of the dehazing algorithms to see the effects on the accuracy of the measured atmospheric scattering coefficient.

Our first observation is that the polarization-based dehazing algorithm suffers with a small error in the degree of polarization (Figure 3). The polarization-based dehazing is naturally dependent on the degree of polarization. When a small error is injected into it, this technique is the most accurate in measuring the atmospheric scattering. When the error in polarization increases slightly, as can be seen in Figure 3, we see a large decrease in the accuracy of the atmospheric scattering. The polarization parameter in the polarization-based dehazing algorithm is a scalar



Figure 2: A sequence of four images of the same scene taken at constant intervals over time. A slight variation in the illumination of the scene is evident.

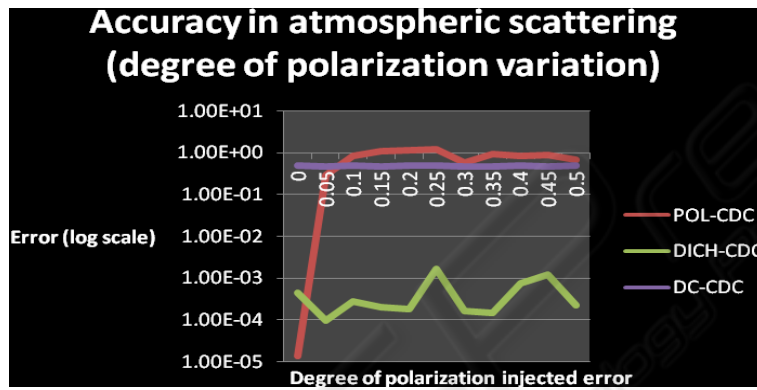


Figure 3: The accuracy of the measured atmospheric scattering of the haze simulations for the three dehazing algorithms as an error in degree of polarization is increased: polarization dehazing with CDC (POL-CDC), dichromatic dehazing with CDC (DICH-CDC) and dark channel dehazing with CDC (DC-CDC). Fluctuations in the methods is due to random generation of the simulated scene radiance.

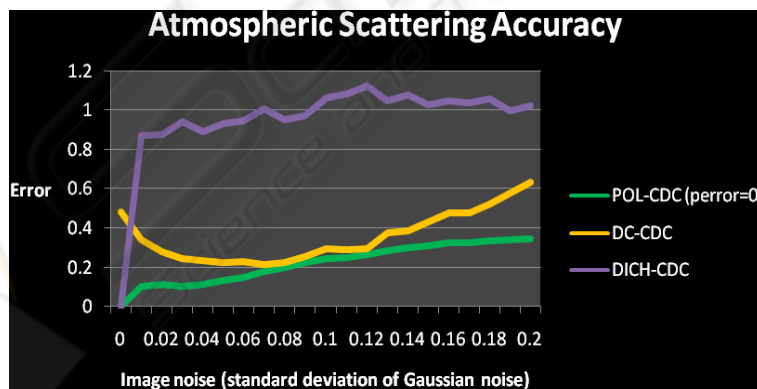


Figure 4: The figure shows the dehazing methods compared to each other. Clearly the dichromatic framework displays the worst performance. The polarization dehazing shows the least error as image noise increases. The dark channel decreases at first with low noise but then rises with high noise. No error is injected into the degree of polarization ($perror = 0$).

value from 0 to 1. The dichromatic framework performs well under no noise but as soon as a small amount of noise is introduced it becomes the least accurate approach falling below the other two algorithms (Figure 4). The dark channel starts off with a larger error than the other two dehazing methods. It initially improves under low noise but then worsens as

noise increases (Figure 4). This unstable trend in the accuracy of the dark channel may be due to the fact that this technique is highly dependent on color information in the images. In some situations the dark channel of a part of the image is not small and negligible. This happens due to surfaces in the image with similar radiance to that of the haze in the scene

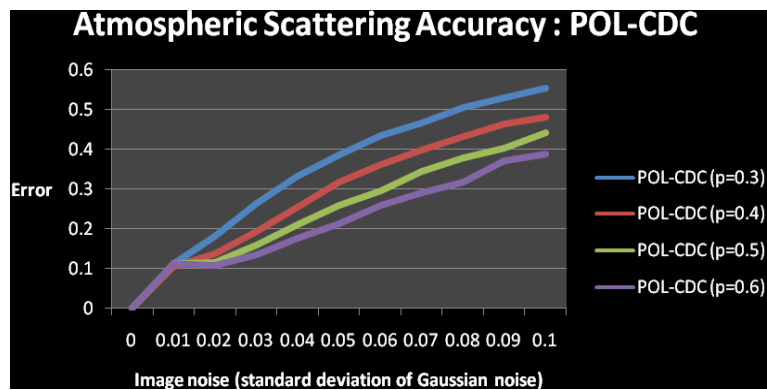


Figure 5: The figure shows the polarization dehazing with CDC (POL-CDC). As the image noise increases the error increases in general. There are four different plots for the POL-CDC with different values of the degree of polarization p .



Figure 6: The two reference regions of the scene used to compute the distance ratio from Google Maps. The distance to the billboard in the scene above is approximately 2.2 km. The distance to the flat surface of the building in the foreground is approximately 493.9 m.

(He et al., 2009). This distorts the accuracy of the measured atmospheric scattering. Therefore increasing image noise greatly affects the color information in the images and hence greatly affects the accuracy of the dark channel method. The polarization dehazing outperforms the other dehazing algorithms as image noise increases and as the degree of polarization varies within realistic bounds we see no significant change in the accuracy of this approach (Figure 5).

In order to verify the accuracy of the unscaled depthmaps recovered by each of the existing dehazing algorithm with and without the CDC extension, we gathered ground truth measurements from Google Maps. We measured the distances between the viewpoint and the two relatively flat regions shown in Figure 6 by locating them on Google Maps. The ratio of these two distances is what we use to compare the relative depthmaps.

As you can see from Table 1, the CDC optimiza-

tion algorithm increases the accuracy of the recovered depthmap by factoring out the atmospheric scattering scalar. This is done by optimizing according to the constraint of constant depth of a scene over time (CDC). For this reason all the dehazing algorithms analyzed are improved when the CDC is applied to its output. The CDC optimization enhances the accuracy of the polarization dehazing algorithm by approximately 4% and enhances the accuracy of the dark channel by approximately 42%. It should be noted that our implementation of the dark channel method does not include the soft matting which does improve the dehazing of this method. This requires further investigation to determine how much more accurate in measuring atmospheric scattering the dark channel method becomes with soft matting applied. Differences between the accuracy of the methods could be due to different unknown scale factors in each dehazing method. For example, the polarization method may introduce linear or non-linear scale factors in the process of filtering the light through the polarizer filter. There are many other unknown scale factors such as: ground-reflection, ambient light, variation in illumination and occlusions. The many possible scale factors are too many to fully account for in the scope of this research.

Table 1: The distance ratio returned by each algorithm averaged across the regions of the image shown in Figure 6.

Algorithm	Distance Ratio
Ground truth (using Google Maps)	4.50
POL	3.55
POL-CDC	3.69
DC	0.59
DC-CDC	0.83

5 CONCLUSIONS

We have presented two contributions in this research. The first is an investigation into dehazing methods to be used for measuring atmospheric scattering from images. We extend each dehazing method to use a sequence of images captured over time. The polarization-based dehazing has initially shown it is the most accurate method provided the degree of polarization is large enough to be detected between the images and there is no significant error in the degree of polarization. The second contribution is the CDC optimization which extends each dehazing algorithms to recovering a more accurate unscaled depthmap of the scene.

There is still much more room for research in this area. One future work can be to correlate the atmospheric scattering to PM levels measured by conventional devices (Eiseman, 1998a; Eiseman, 1998b). More dehazing methods should be investigated and compared to the three dehazing algorithms we have analyzed in this research. More research can be done in separating the two parts of haze (natural molecular and PM parts) to more accurately determine the level of PM from images. Other visual data can be analyzed to measure atmospheric scattering such as video streams. The methods of measuring depth and atmospheric scattering recovered can be applied to further dehaze the scene more accurately.

REFERENCES

- Eiseman, E. (1998a). Appendix a: Air monitoring technologies for particulate matter. Technical report, Critical Technologies Institute - RAND Corporation.
- Eiseman, E. (1998b). Appendix b: Examples of air monitoring technologies for particulate matter. Technical report, Critical Technologies Institute - RAND Corporation.
- Fattal, R. (2008). Single image dehazing. *ACM Trans. Graph.*, 27(3).
- He, K., Sun, J., and Tang, X. (2009). Single image haze removal using dark channel prior. In *CVPR09*, pages 1956–1963.
- Jacobson, M. Z. (2005). *Fundamentals of Atmospheric Modeling*. Cambridge University Press, 2nd edition.
- Kokhanovsky, A. (2003). *Polarization Optics of Random Media*. Jointly published with Praxis Publishing.
- Kopf, J., Neubert, B., Chen, B., Cohen, M., Cohen-Or, D., Deussen, O., Uyttendaele, M., and Lischinski, D. (2008). Deep photo: Model-based photograph enhancement and viewing. *ACM Transactions on Graphics (Proceedings of SIGGRAPH Asia 2008)*, 27(5):116:1–116:10.
- Narasimhan, S. and Nayar, S. (2000). Chromatic Framework for Vision in Bad Weather. In *IEEE Conference on Computer Vision and Pattern Recognition (CVPR)*, volume 1, pages 598–605.
- Narasimhan, S. and Nayar, S. (2002). Vision and the atmosphere. *IJCV*, 48(3):233–254.
- Narasimhan, S. and Nayar, S. (2003). Interactive (De)weathering of an Image using Physical Models. In *ICCV Workshop on Color and Photometric Methods in Computer Vision (CPMCV)*.
- Schechner, Y., Narasimhan, S., and Nayar, S. (2003). Polarization-based vision through haze. *AppOpt*, 42(3):511–525.
- Shwartz, S., Namer, E., and Schechner, Y. (2006). Blind haze separation. In *CVPR06*, pages II: 1984–1991.
- Tan, R. (2008). Visibility in bad weather from a single image. In *CVPR08*, pages 1–8.
- Vollmer, M. (2003). A simple method for estimating the thickness of the atmosphere by light scattering. *Am. J. Phys.*, 71(10).